Communications Research Centre

RANGE ESTIMATION
FROM WAVE-FRONT CURVATURE

by

R.V. Webber

DEPARTMENT OF COMMUNICATIONS
MINISTÈRE DES COMMUNICATIONS

CRC REPORT NO. 1322

CANADA

OTTAWA, MARCH 1979
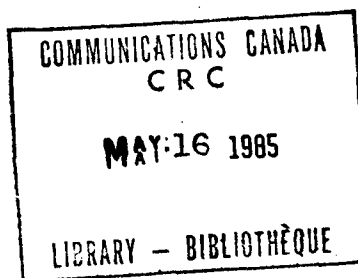
COMMUNICATIONS RESEARCH CENTRE

DEPARTMENT OF COMMUNICATIONS

CANADA

RANGE ESTIMATION FROM WAVE-FRONT CURVATURE

by

R.V. Webber

(Radio and Radar Research Branch)

CRC REPORT NO. 1322

March 1979

OTTAWA

TABLE OF CONTENTS

RANGE ESTIMATION FROM WAVE-FRONT CURVATURE

by

R.V. Webber

ABSTRACT

The computation of the range of a signal from its wavefront curvature has been investigated. Some success was obtained by fitting a truncated power series to phase data which was taken by a linear array of antenna. In simulated experiments the effect of noise in the data was investigated extensively. For typical data obtained with the Communications Research Centre HFDF 1.2 km array, one should be able to make useful estimates of range for distances up to about 100 kilometers.

In a field experiment the ground wave was used to estimate ranges of up to 111 kilometers. The bias and the rms deviation from the mean range were low for the near transmission sites but were up to 33% and 45% respectively, for the more remote sites. An unsuccessful attempt was made to compute the range of a signal which had been reflected by the E layer of the ionosphere. In this case the range was about twice the useful limit for the present system and the received signal may well have consisted of two or more interfering rays.

Because of distorted wavefronts resulting from wave interference the range cannot be computed for a resultant signal which is made up of two or more signals which come from almost the same direction.

1. INTRODUCTION

The question of the ability of a linear antenna array to measure the range of a transmitter from the curvature of the wavefront is one that is raised periodically. In this study a method will be presented for carrying

2

out such a range calculation. Some of the limits on the technique will be investigated theoretically and it will be tested both with simulated data and with data which were collected on the CRC HFDF system.

Rice and Winacott[1] have described the HFDF array which has an aperture of 1181.1 meters. Phases are measured along the array relative to the phase at one end of the array. The expected error due to the instrumentation in the measured value of the phase at each antenna is ±3 degrees for all frequencies in the bandwidth 2 – 30 MHz. The range at which a transmitter, located broadside to the array, produces a 3 degree phase difference between the ends and the centre of the array due to wavefront curvature varies from 140 km at 2 MHz to 1400 km at 20 MHz. Thus, with sufficient signal to noise ratio, it would be reasonable to expect to be able to measure up to these ranges at the corresponding frequencies.

A necessary condition is that there be measurable curvature in the result when phase, θ, is plotted against distance along the array, x, and the higher the curvature the better. Because of this such a method would work best for a signal incident from directions near broadside and would not work at all for a signal with an endfire direction. This is shown in Figure 1. Figure 1(a) shows three possible orientations of an array with respect to the transmitter. Figure 1(b) shows representative plots of phase against distance along the array. The correspondence between the array positions and the plots is indicated by numbers. For positions 1 and 3, both endfire positions, there is no curvature in the plot. For position 2, a broadside position, the curvature is maximum. Also, as range increases the wavefront becomes more planar so the method will become less reliable as range increases to large values.
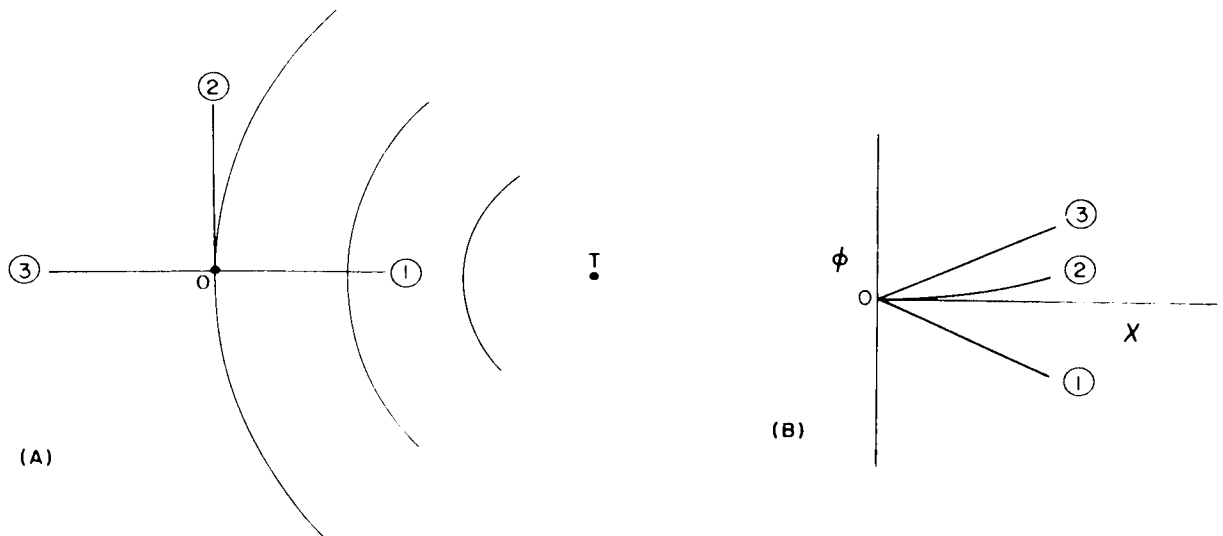

Figure 1. Diagrams to Show Relationship Between Orientation of Array and the Plot of Radio-Wave Phase Against Distance x

2. THEORY

The method which was used to estimate range and direction will be explained with the aid of Figure 2. In that figure the point T represents the location of a transmitter. The line OP represents a linear array of antennas. The line OT represents the range, R, of the transmitter with respect to a reference antenna at the end of the array which is represented by the point O, and θ represents the direction of the transmitter with respect to the same antenna and the line through the array. The line xT represents the distance, C_x, from the transmitter to an arbitrary antenna at x where x is the distance along the array from the reference antenna.

The phase path different, C_x-R, was expressed as a function of x, $f(x)$, and then expanded in a MacLauren series, i.e.

$$f(x) = \{R^2 + x^2 - 2Rx \cos \theta\}^{\frac{1}{2}} - R \tag{1}$$

The MacLauren series is

$$f(x) = f(0) + f'(0) \, x + \frac{f''(0)}{2} \, x^2 + \dots \tag{2}$$

where, from equation (1)

$$f(0) = 0 \tag{3}$$

$$f'(0) = -\cos \theta \tag{4}$$

$$f''(0) = \frac{\sin^2 \theta}{R} \tag{5}$$

$$f'''(0) = \frac{3 \cos \sin^2\theta}{R^2} \tag{6}$$
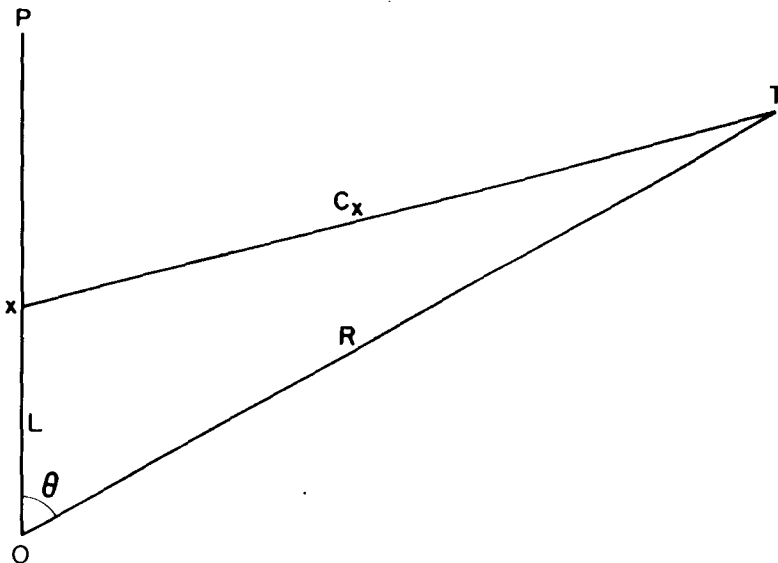

Figure 2. Diagram to Show Method of Estimating Range and Direction

It may be noted that $f'(0)$ is a function of θ only while $f''(0)$ and all higher derivations are functions of both θ and R. Thus to find θ and R it is necessary to determine only $f'(0)$ and $f''(0)$.

Since the elements of the array are equally spaced we may write

$$x_i = id \tag{7}$$

where x_i is the distance from antenna 0 to antenna i, d is the inter-element spacing and i is either zero or a positive integer. Series (2) may now be written as

$$f(x_i) = f(0) + f'(0)di + \frac{f''(0)}{2} d^2 i^2 + \ldots \tag{8}$$

or

$$y_i = \frac{f(x_i)}{d} = \frac{f(0)}{d} + f'(0)i + \frac{f''(0)}{2} di^2 + \ldots \tag{9}$$

where y_i will be identified with normalized phase path data obtained from measurements along a linear array. Normalization here implies division by the antenna spacing.

To y_i is now fitted, by least squares, the series

$$y = a_o + a_1 i + a_2 i^2 + a_3 i^3 + \ldots + a_M i^M \tag{10}$$

If M terms are used, series (10) is fitted to the normalized phase path data by solving the equations

$$
\left.
\begin{aligned}
a_o T_o + a_1 T_1 + a_2 T_2 + \ldots + a_M T_M &= Y_o \\
a_o T_1 + a_1 T_2 + a_2 T_3 + \ldots + a_M T_{M+1} &= Y_1 \\
a_o T_2 + a_1 T_3 + a_2 T_4 + \ldots + a_M T_{M+2} &= Y_2 \\
 \cdot \\
 \cdot \\
 \cdot \\
a_o T_M + a_1 T_{M+1} + a_2 T_{M+2} + \ldots + a_M T_{2M} &= Y_M
\end{aligned}
\right\} \tag{11}
$$

where

$$T_j = \sum_{i=0}^{N-1} i^j , \tag{12}$$

$$Y_j = \sum_{i=0}^{N-1} y_i i^j , \tag{13}$$

0^0 is defined as unity and N is the number of antennas in the array.

These equations are derived in Appendix A.

The value M = 2 was used in most applications of equation (11). This will be justified later when the simulated experiments are described.

If there are no errors in the data

$$a_1 = -\cos \theta \tag{14}$$

or

$$\theta = \cos^{-1}(-a_1) \tag{15}$$

and

$$a_2 = \frac{\sin^2\theta \ d}{2R} \tag{16}$$

or

$$R/d = \frac{\sin^2\theta}{2a_2} \tag{17}$$

$$= \frac{1 - a_1^2}{2a_2} \tag{18}$$

Thus θ may be computed from a_1 of series (10) and R/d may be computed from a_1 and a_2 of that series.

In the practical case equations (15) and (18) will be only approximations because of errors in the data and because series (10) is necessarily truncated.

3. SIMULATION EXPERIMENTS TO FIND THE OPTIMUM VALUE OF M

To find out what value of M is the best to use in series (10), some simulation experiments were carried out in which the value of M varied from 2 to 5. Perfect data were generated by the computer; series (10) was fit to these data by least-squares-best-fit and values for θ and R/d were computed by equations (15) and (18). The results for various normalized ranges and directions are shown in the fourth column of Table 1. The normalized range tended to be computed more accurately for θ values of 90° and for the higher order series. The errors in the values computed for θ were sometimes as much as 0.2 degrees for a second order series and for the lowest normalized range used. Otherwise the error in direction was not greater than 0.01 degrees. The errors tended to be least for the longer ranges.

In another set of experiments random gaussian errors with a standard deviation of 0.01 were incorporated into the normalized data. (This error corresponds to a phase error of 2.3 degrees at 5 MHz on the CRC HFDF

TABLE 1

Results of Computations to Find Optimum Order of Series

Normalized Range	θ (Deg)	Order of Series	Normalized Range Found	
			S.D. = 0	S.D. = 0.01
200	90°	2	202	205
		3	199	191
		4	200	204
		5	200	206
200	30°	2	160	170
		3	205	175
		4	200	219
		5	200	225
2000	90°	2	2.00×10^3	2.36×10^3
		3	2.00×10^3	1.42×10^3
		4	2.00×10^3	2.55×10^3
		5	2.00×10^3	2.75×10^3
2000	30°	2	1.96×10^3	4.92×10^3
		3	2.00×10^3	7.54×10^3
		4	2.00×10^3	1.46×10^4
		5	2.00×10^3	neg.
20,000	90°	2	2.00×10^4	neg.
		3	2.00×10^4	3.92×10^3
		4	2.00×10^4	neg.
		5	2.00×10^4	neg.
20,000	30°	2	2.00×10^4	neg.
		3	2.00×10^4	$1.14 \times .10^3$
		4	2.00×10^4	neg.
		5	2.00×10^4	neg.

system.) The computed values for the normalized range are in Column V of Table 1. The estimates of range are better for the lower ranges than for the higher ones. However, the higher order series gave no better estimates of range than the second order series. Therefore, unless otherwise stated, the value M = 2 was used in all the remaining computations which are reported in this paper.

4. ERROR ANALYSIS FOR GAUSSIAN PHASE ERRORS

An error analysis will be performed for M = 2 to see what to expect from the subsequent data analysis. First it will be shown that the parameters a_o, a_1 and a_2 are linear functions of the $\{y_i\}$. This allows the calculation of expected values and standard deviations for a_o, a_1 and a_2.

For the case M = 2 equations (11) take the form

$$a_o T_o + a_1 T_1 + a_2 T_2 = Y_o$$

$$a_o T_1 + a_1 T_2 + a_2 T_3 = Y_1 \tag{19}$$

$$a_o T_2 + a_1 T_3 + a_3 T_4 = Y_2$$

or

$$\overline{Q}\overline{A} = \overline{Y} \tag{20}$$

where

$$\overline{Q} = \begin{pmatrix} T_0 & T_1 & T_2 \\ T_1 & T_2 & T_3 \\ T_2 & T_3 & T_4 \end{pmatrix}, \tag{21}$$

$$\overline{A} = (a_o\ a_1\ a_2)^T, \tag{22}$$

and

$$\overline{Y} = (Y_o\ Y_1\ Y_2)^T, \tag{23}$$

where the superscript T means transpose and the bar over a symbol (e.g., $\overline{Q}$) indicates a matrix or a vector.

Now

$$Y_j = \sum_{i=0}^{N-1} i^j y_i \tag{24}$$

$$= C_j^T \overline{P} \tag{25}$$

where

$$\overline{C}_j = (0^j\ 1^J\ \ldots\ (N-1)^j)^T, \tag{26}$$

and $\overline{P}$

$$\overline{P} = (y_o y_1\ \cdot\ \cdot\ \cdot\ y_{N-1})^T \tag{27}$$

But

$$a_o = W_1 Y_o - W_2 Y_1 + W_3 Y_2 \tag{28}$$

where W_1, W_2 and W_3 are the determinants of minors of $\overline{Q}$ divided by the determinant of $\overline{Q}$. Equation (28) may now be written

$$a_o = W_1 \bar{C}_o^T \bar{P} - W_2 \bar{C}_1^T \bar{P} + W_3 \bar{C}_2^T \bar{P} \tag{29}$$

$$= (W_1 \bar{C}_o^T - W_2 \bar{C}_1^T + W_3 \bar{C}_2^T) \bar{P} \tag{30}$$

The last equation may be written

$$a_o = (Z_{01} \; Z_{02} \; \cdots \; Z_{0N}) \bar{P} \tag{31}$$

where

$$Z_{o\ell} = W_1 C_{o,\ell} - W_2 C_{1,\ell} + W_3 C_{2,\ell} \tag{32}$$

where $C_{j,\ell}$ is the ℓth component of $\bar{C}_j$. Hence a_o is a linear function of the $\{y_i\}$.

If it is assumed that the errors in each y_i follow the same Gaussian distribution which has a mean of zero and a variance of σ_y^2, then the expected value of each y_i is just that value which it would have if it contained no errors. The expected value of a_o is then

$$E(a_o) = (Z_{01} \; Z_{02} \; \cdots \; Z_{0N}) \; E(\bar{P}) \tag{33}$$

which, in the case of simulated data, may be computed by using the data without adding any noise to it.

Further from equation (31) the variance of a_o, $\sigma_{a_o}^2$, may be computed from the expression.

$$\sigma_{a_o}^2 = (Z_{01}^2 + Z_{02}^2 + \ldots Z_{0N}^2) \; \sigma_y^2 \tag{34}$$

Also, the probability density function of a_o, $p(a_o)$, will be gaussian.

In a similar way the expected values and the variances of a_1 and a_2 may be found so that

$$E(a_1) = (Z_{11} \; Z_{12} \; \ldots Z_{1N}) \; E(\bar{P}) \tag{35}$$

$$\sigma_{a_1}^2 = (Z_{11}^2 + Z_{12}^2 + \ldots + Z_{1N}^2) \; \sigma_y^2 \tag{36}$$

$$E(a_2) = (Z_{21} \; Z_{22} \; \cdots \; Z_{2N}) \; E(\bar{P}) \tag{37}$$

$$\sigma_{a_2}^2 = (Z_{21}^2 + Z_{22}^2 + \ldots Z_{2N}^2) \; \sigma_y^2 \tag{38}$$

Also $p(a_1)$ and $P(a_2)$ will both be gaussian probability density functions.

It may be noted that, in equations (33) to (38), the Z_{ij} are functions of the number of antennas only so that σ_{a_o}, σ_{a_1} and σ_{a_2} are independent of either range or direction.

It will now be shown that $E(a_1)$ and $E(a_2)$ are not independent. As already noted $E(a_1)$ and $E(a_2)$ are the values which would be obtained for a_1 and a_2 if there were no errors in the phase measurements. Then for a given frequency these parameters are functions only of the orientation of the array with respect to the transmitter. Referring again to Figure 1(b) it may be seen that for position (1) the curvature is zero for the plot of phase against x and that the slope (at antenna zero) is a minimum, i.e., most negative. For that position then a_2 is zero and a_1 is a minimum. For position (2) the curvature is a maximum and the slope at antenna zero is zero, so a_1 is zero and a_2 is a maximum. For position (3) the curvature is again zero while the slope is a maximum so a_2 is again zero while a_1 is a maximum. Thus the values of these two parameters are related and are not independent.

The errors in a_1 and a_2, which are caused by errors in the phase data are not independent either. In Figure 3 let curve (1) be a true plot of y against x, i.e., with no errors in the phase data. Errors in the data will cause the least-squares-best-fit curve to deviate from the true curve. Let curve (2) be such a possible curve. For this curve the curvature is increased so that a_2 is increased. However, the slope at antenna zero is unchanged so a_1 is unchanged. Curve (3) has the same curvature as curve (2). Curve (3), however, gives a better least-squares-best-fit to the true curve, curve (1), than does curve (2). To get this better fit the slope of the curve at antenna zero had to change so that a_1 had to change (in this case a_1 decreased). Thus the errors in a_1 and a_2 are related and are not independent.
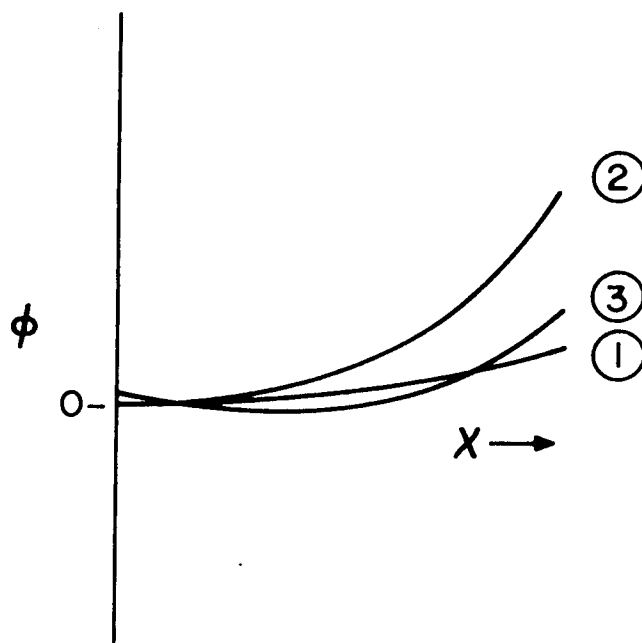

Figure 3. Diagram to Show that a_1 and a_2 are not Statistically Independent

It would be desirable to be able to compute an expected value and a variance for the computed value of R/d. This, however, is impossible. One may write formally

$$E(\frac{R}{d}) = \int\int (\frac{1-a_1^2}{2a_2}) \; p(a_1,a_2) \; da_1 \; da_2 \tag{39}$$

But a_2 can be zero in which case the integrand of equation (3) is infinite so the integral is infinite. Therefore R/d does not have a finite expected value. Similarly R/d does not have a finite variance.

5. WAVE INTERFERENCE

It may be seen from equation (18) that the sign on the computed value of R/d is the same as the sign on a_2. Reference to equation (10), for M = 2, shows that if R/d is to be positive then the plot of phase as a function of antenna position must curve upward. If the curvature is downward a negative value will be obtained for $\frac{R}{d}$. Studies of the phase distribution of two interferring signals have been made by Haydon[2]. It was shown that the curvature of the wavefront over a limited aperture could be either positive or negative. Hence, the method devised here for estimating range may fail if two (or more) signals are received at the same time.

6. CHECKING THE ERROR ANALYSIS BY SIMULATION EXPERIMENTS

Equations (35) to (38) were tested empirically by computer simulation experiments. In these experiments data were generated in the computer for a given normalized range and direction. Gaussian random errors of a given standard deviation were then added. From these data a_1 and a_2 were computed. This was repeated 100 times. For these 100 values of a_1 and a_2 the mean a_1, a_{1M}, the rms deviation of a_1 from its mean, RMSD a_1, the mean a_2, a_{2M}, and the rms deviation of a_2 from its mean, RMSD a_2, were computed. $E(a_1)$, σ_{a_1}, $E(a_2)$ and σ_{a_2} were computed by equations (35) to (38). The results for $\theta = 80°$, $\sigma_y = 0.005$ and various values of R/d are given in Table 2. It may be noted that $E(a_1)$ is independent of range; (it is a function of direction only) and that there is agreement to 3 significant figures between $E(a_1)$ and a_{1M}. Also σ_{a_1} and σ_{a_2} are independent of range as expected. The agreement between σ_{a_1} and RMSD a_1 is not perfect but it appears to be within acceptable limits; it is also small when compared with $E(a_1)$. There is close to perfect agreement between $E(a_2)$ and a_{2M}. The agreement between σ_{a_2} and RMSD a_2 is also acceptable. These results confirm that the method of estimating R/d and θ is working properly.

It may be noted that, at least for directions near broadside to the array, and for the array configuration used here, the standard deviation of the estimated direction-of-arrival θ, is about 3.7 times larger than would

TABLE 2

Sample Print-Out of Simulation Experiments

θ	σ_y	R/d	$E(a_1)$		a_{1M}		σ_{a_1}	RMSD a_1	$E(a_2)$	a_{2M}	σ_{a2}	RMSD a_2
80.	.0050	200	-.174E	00	-.174E	00	.372E-03	.461E-03	.250E-02	.250E-02	.116E-04	.116E-04
80.	.0050	500	-.174E	00	-.174E	00	.372E-03	.305E-03	.984E-03	.985E-03	.116E-04	.110E-04
80.	.0050	1000	-.174E	00	-.174E	00	.372E-03	.444E-03	.489E-03	.487E-03	.116E-04	.103E-04
80.	.0050	1500	-.174E	00	-.174E	00	.372E-03	.453E-03	.325E-03	.325E-03	.116E-04	.120E-04
80.	.0050	2000	-.174E	00	-.174E	00	.372E-03	.440E-03	.243E-03	.242E-03	.116E-04	.117E-04
80.	.0050	3000	-.174E	00	-.174E	00	.372E-03	.266E-03	.162E-03	.161E-03	.116E-04	.116E-04
80.	.0050	4000	-.174E	00	-.174E	00	.372E-03	.376E-03	.121E-03	.121E-03	.116E-04	.967E-05
80.	.0050	6000	-.174E	00	-.174E	00	.372E-03	.444E-03	.809E-04	.802E-04	.116E-04	.104E-04
80.	.0050	8000	-.174E	00	-.174E	00	.372E-03	.386E-03	.607E-04	.598E-04	.116E-04	.108E-04
80.	.0050	10000	-.174E	00	-.174E	00	.372E-03	.366E-03	.485E-04	.488E-04	.116E-04	.113E-04

be expected from the simpler procedure of fitting a straight line to phase data under a plane-wave-plus-Gaussian-noise assumption[1]. The larger standard deviation arises in the present case because the procedure used here allows more degrees of freedom by estimating both a slope (at the origin) and curvature, rather than just an average slope over all the spatial data.

7. COMPUTATIONS USING SIMULATED DATA

The term "percent bias" is used in the next paragraph. It is defined as follows. Let S be the sample mean of a quantity, i.e., the average of the computed values of that quantity, and let V be the true value of that quantity. Then

$$\text{Bias} = S - V \tag{40}$$

and

$$\text{percent bias} = \frac{\text{bias} \times 100}{V} \tag{41}$$

Figure 4 shows the percent bias on the estimated values of R/d when R/d is computed from a_{1M} and a_{2M}. The two curves ($\sigma_y = 0.01, 0.003$) merge for R/d < 500. The small but finite % bias for R/d = 200 is due to the use of M = $\overline{2}$ (when the value M = 3 was used this % bias decreased). Otherwise the two curves appear to vary randomly about zero. The curve for $\sigma_y = 0.01$ is mostly above zero, but this is not believed to be significant.

Although theoretical values for E(R/d) and $\sigma_{R/d}$ do not exist, estimates can be made under certain conditions of a pseudo-$E(\frac{R}{d})$ and a pseudo-$\sigma_{R/d}$. This is done by computing R/d for a large number of simulated cases and finding the mean R/d, as an estimate of $E(\frac{R}{d})$ and the rms deviation of R/d from its mean, as an estimate of $\sigma_{R/d}$. The difficulty is that if a_2 is positive but near zero the resulting value of R/d is very large and if a_2 is negative the resulting value of R/d is negative. This situation may be avoided if a_2 is kept much larger than zero. That this can be done most of the time may be seen in Figure 5. There the gaussian curve represents a possible curve for $p(a_2)$. Since σ_{a_2} does not depend on range the width of
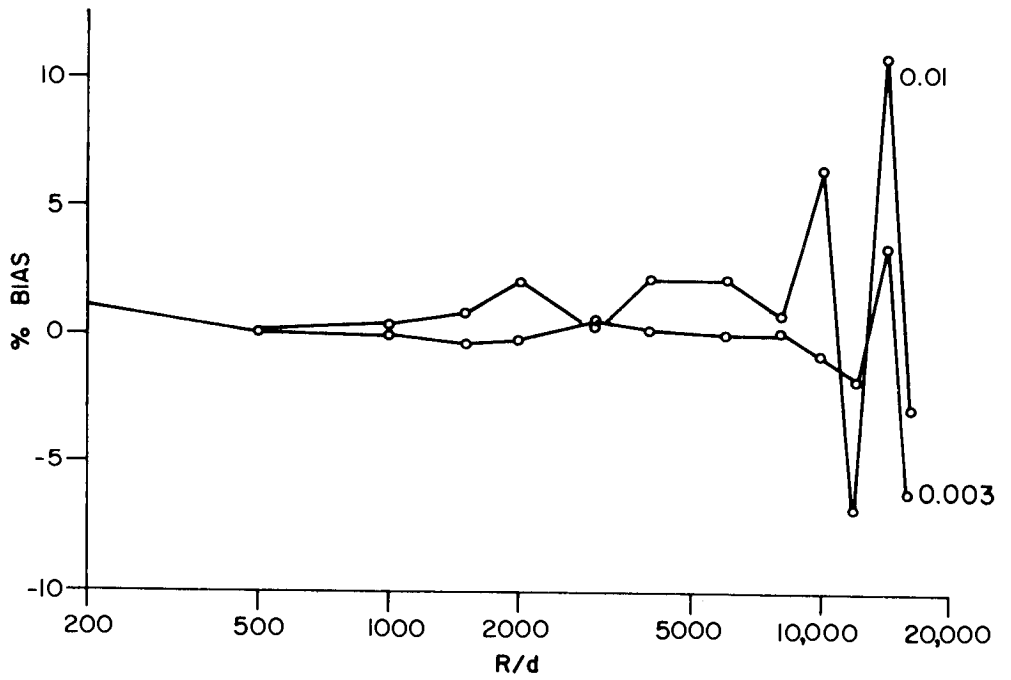
Figure 4. Plot of Percent Bias Against R/d for Computation of R/d from A_{1M} and a_{2M}
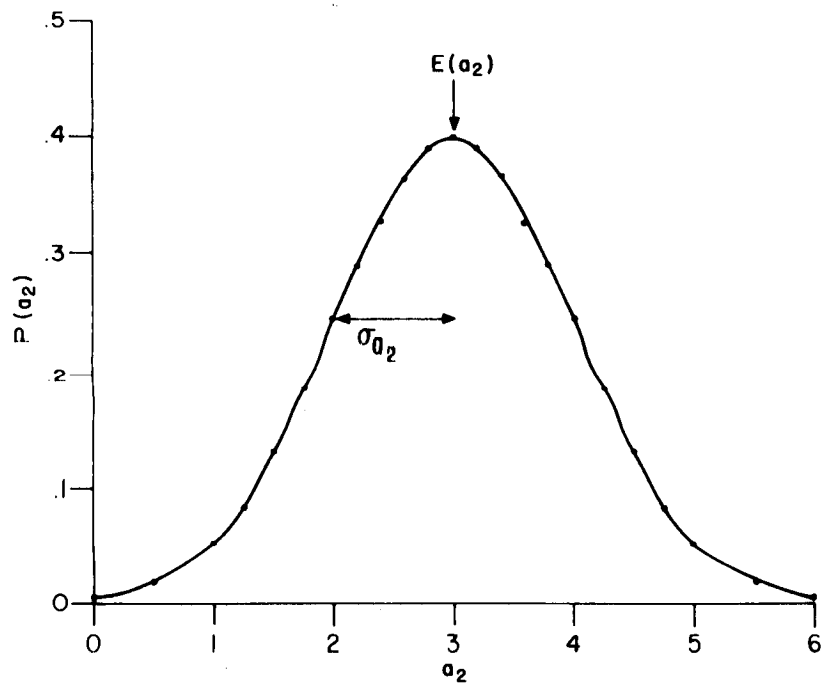

Figure 5. Sketch of $p(a_2)$, the Probability Density Function for a_2

the curve does not change with range. However, as the range increases to infinity the curve moves to the left so that $E(a_2)$ approaches zero. As range decreases the curve moves to the right. For the curve shown in Figure 4 $E(a_2)$ equals 3 times σ_{a_2}. In this case only 0.15% of the distribution falls below zero so that a_2 would be expected to fall below zero only once or twice in a thousand cases. If the curve is moved to the right so that $E(a_2) = 4\sigma_{a_2}$ then only about 0.01 percent of the distribution falls below zero. Since $E(a_2)$ and σ_{a_2} can both be computed theoretically, it is known when the separation between zero and $E(a_2)$ is within a given multiple of σ_{a_2}.

Simulated experiments were carried out to estimate values for $E(\frac{R}{d})$ and $\sigma_{R/d}$ by this method. For given values of R/d, θ and σ_y one hundred sets of data were generated and R/d was estimated for each set. The mean, and the rms deviation from the mean, of the estimated values for R/d were then computed. When the restriction $E(a_2) \geq 3\sigma_a$ was applied, a_2 was sometimes negative for the longest ranges. When the restriction $E(a_2) \geq 4\sigma_{a_2}$ was applied a_2 was positive in all cases. In Figure 6 the percent bias is plotted as a function of R/d for three values of σ_y. As in Figure 5 all curves merge for low values of R/d and there is a small but definite percent bias for the lowest value of R/d which is due to the use of M = 2 in series (10). For the higher values of R/d the three curves separate but all of them are almost always positive. In Figure 7 the rms deviation from the mean is given for five values of σ_y. These curves then, Figures 6 and 7, may be used to predict the outcome of an estimate of R/d. Once in a while however, about once in ten thousand times, a_2 may be near zero, or negative, in which case the estimated value of R/d will be wild. These curves, of course, are valid only for a gaussian distribution of errors in the phase measurements.
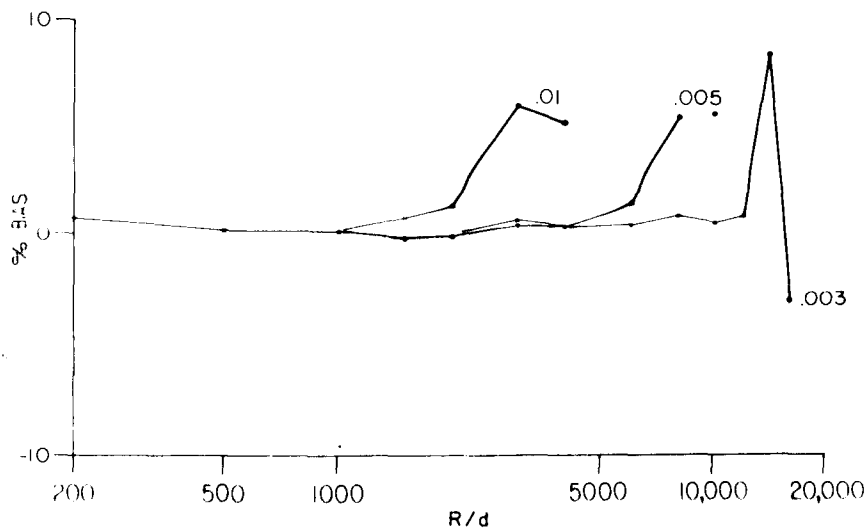

Figure 6. Plot of Percent Bias Against R/d for Various Values of σ_y. Mean R/d found from invidivual Computations of R/d from a_1 and a_2.
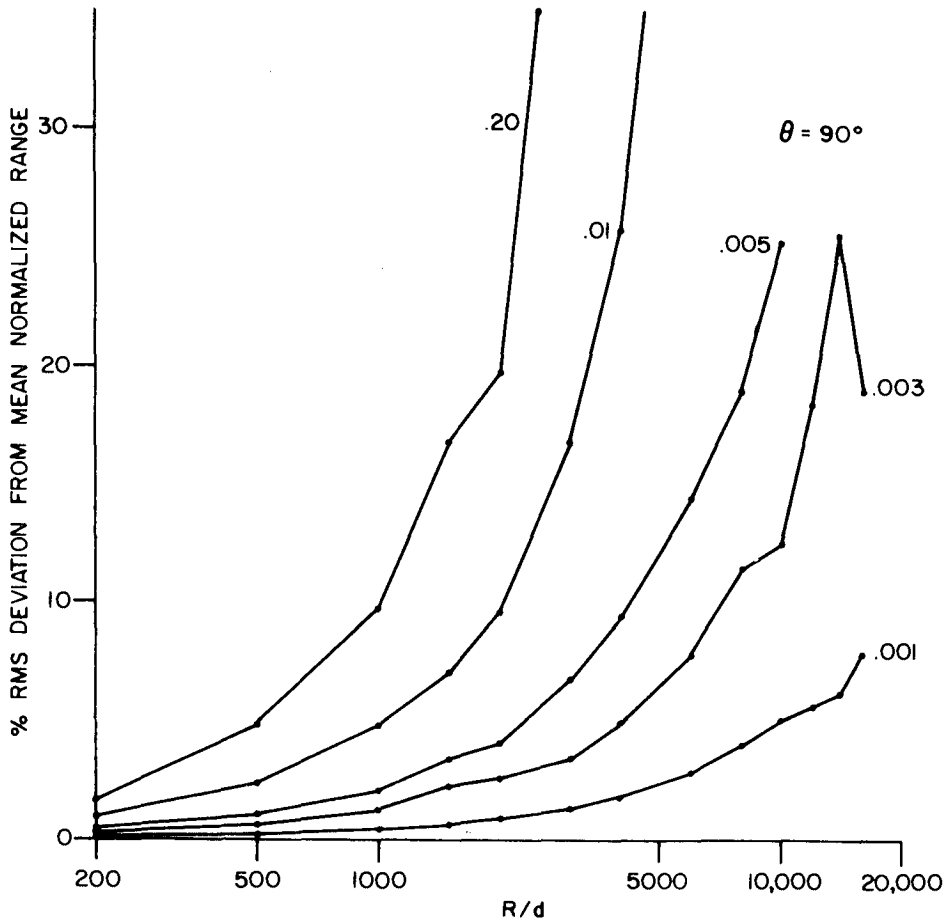
Figure 7. Rms Deviation from Mean Normalized Range Plotted as a Function of True R/d for Various Values of σ_y

8. COMPUTATIONS USING REAL GROUND-WAVE DATA

8.1 THE EXPERIMENT

The method described in this report of determining range and direction was tested under real conditions for ranges up to 111 kilometers. A frequency modulated continuous wave (FMCW) system was used which made it possible to select the ground wave and to eliminate the sky wave on the basis of their respective travel times. Thus the signal which was used was not reflected by the ionosphere. The linear antenna array of 27-foot monopoles at the CRC HFDF site was used to receive the signals. For this experiment the array was made up of 32 elements at 125 feet (38.1 meters) spacing for a total length of 3875 feet (1181.1 meters).

The sites from which the transmissions were sent were chosen to be near a line which ran north-east from the center of the antenna array and which

was perpendicular to the array. The latitude and the longitude of the sites could be estimated, from a large scale map, to about two seconds or about 60 meters. The ranges and the directions of the sites, with respect to the center of the array, were computed by a standard navigation formula.

Since the method used found range and direction with respect to one end of the antenna array, it was necessary to find the actual directions with respect to that end of the array as well. This was done by adding a correction which was computed by the formula,

$$\text{Correction to direction} = (\frac{590.5 \times 57.3}{\text{range}}) \text{ degrees} \qquad (42)$$

In this formula 590.5 meters is one half the length of the array and 57.3 is the number of degrees in a radian.

For all sites which were used, the range from the center of the array did not differ significantly from the range from the end of the array. Therefore, no correction was made to the ranges of the sites.

The ranges and the directions of the transmission sites are given in Table 3.

TABLE 3

Ranges and Directions of Transmission Sites

Site	Range (km)	Direction With Respect to Center of Array (Deg.)	Direction With Respect to End of Array (Deg.)
1	13.38	90.85	93.38
2	21.69	90.78	92.32
3	37.42	91.01	91.91
4	56.46	90.90	91.50
5	74.15	90.53	90.99
6	87.42	90.33	90.72
7	111.46	90.78	91.08

For each site from 7 to 12 transmissions and recordings were made at one minute intervals. For up to ten of these transmissions the phase of the ground wave was plotted as a function of antenna position. Figures 8 and 9 show the plots for site one (range = 13.38 km) for 3.25 and 10.35 MHz respectively. Figures 10 and 11 are similar plots for site seven (range = 111.46 km). Plots for the intermediate sites showed a uniform transition from the plots for site one to the plots for site seven.
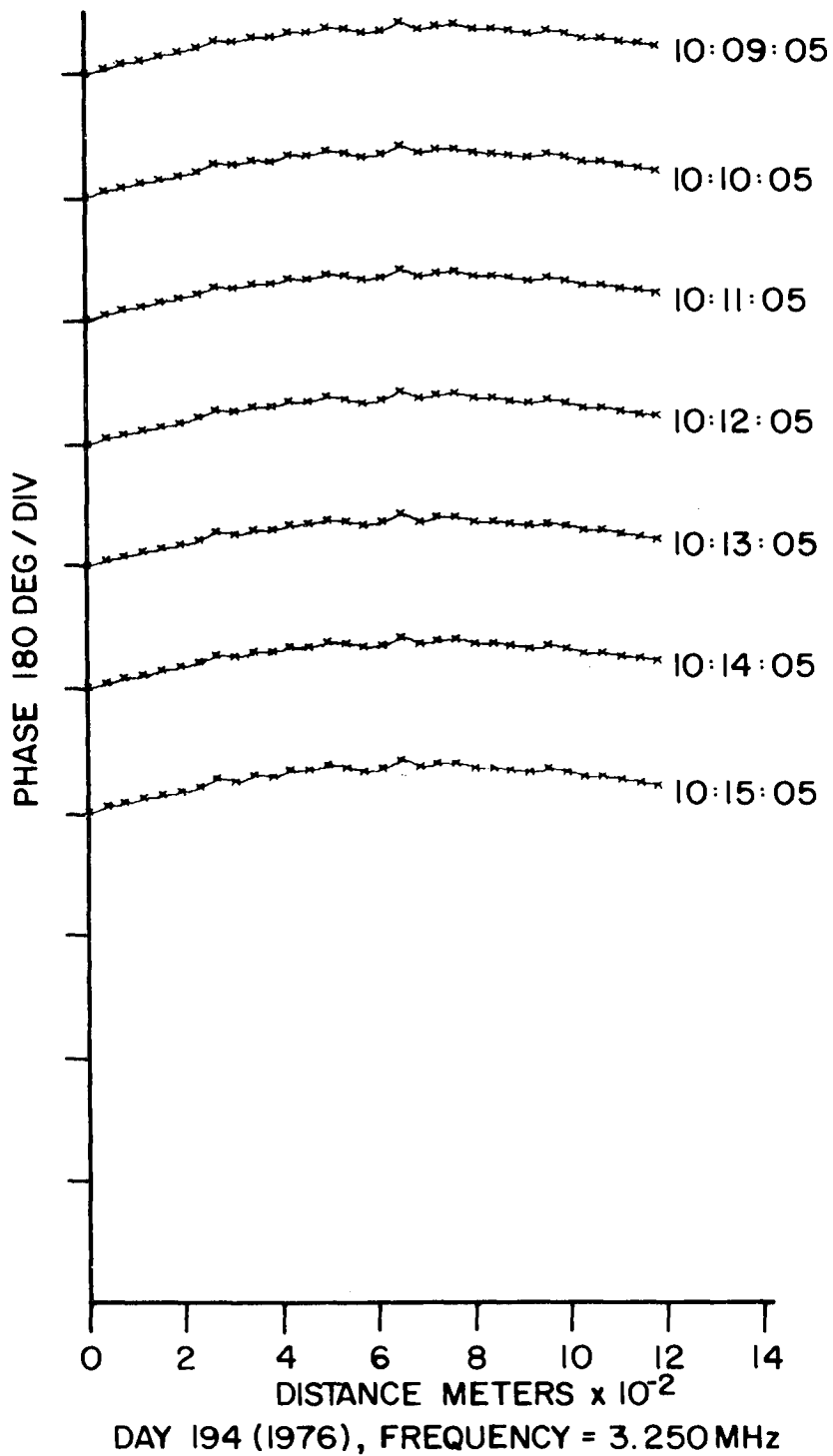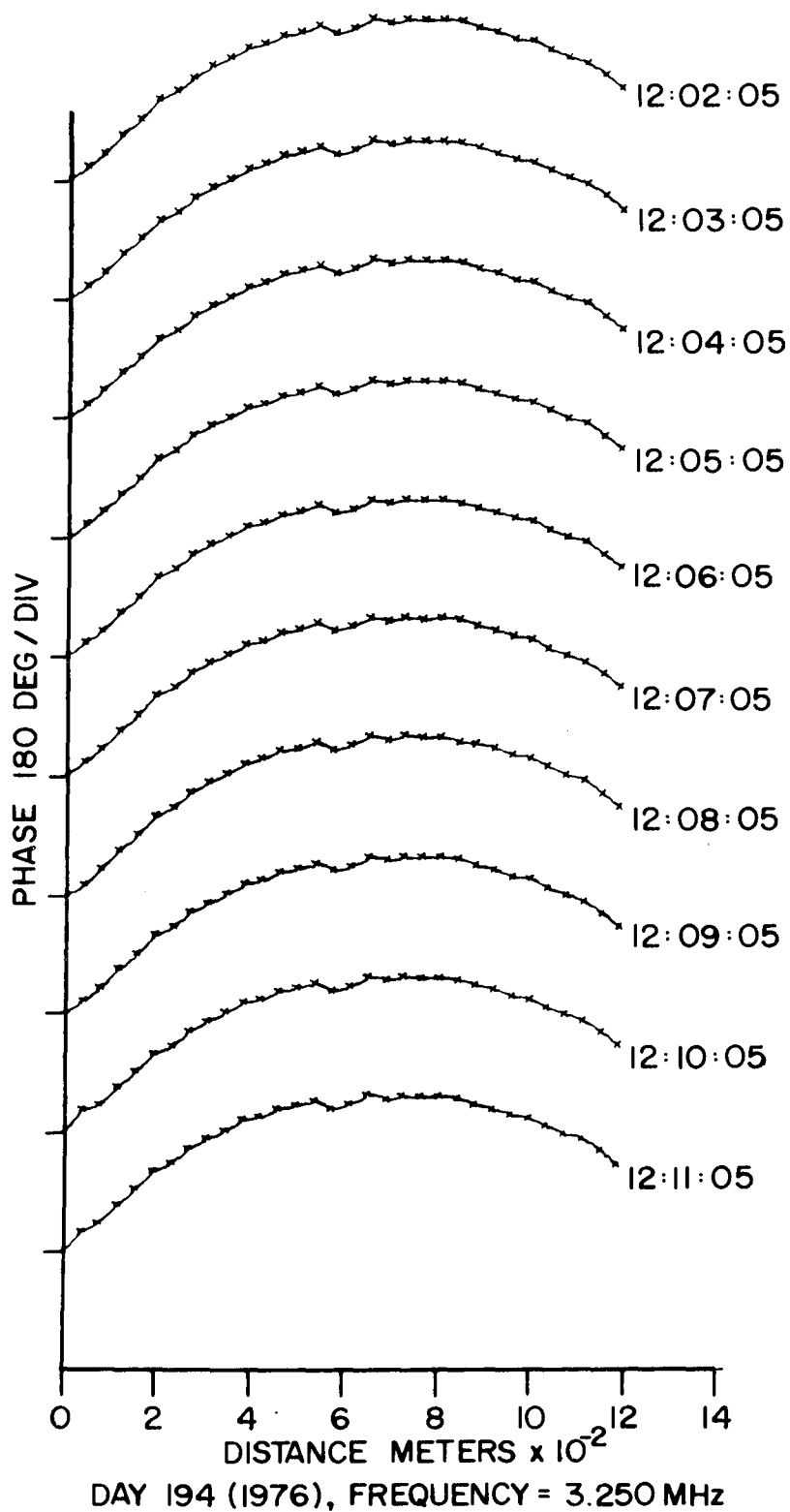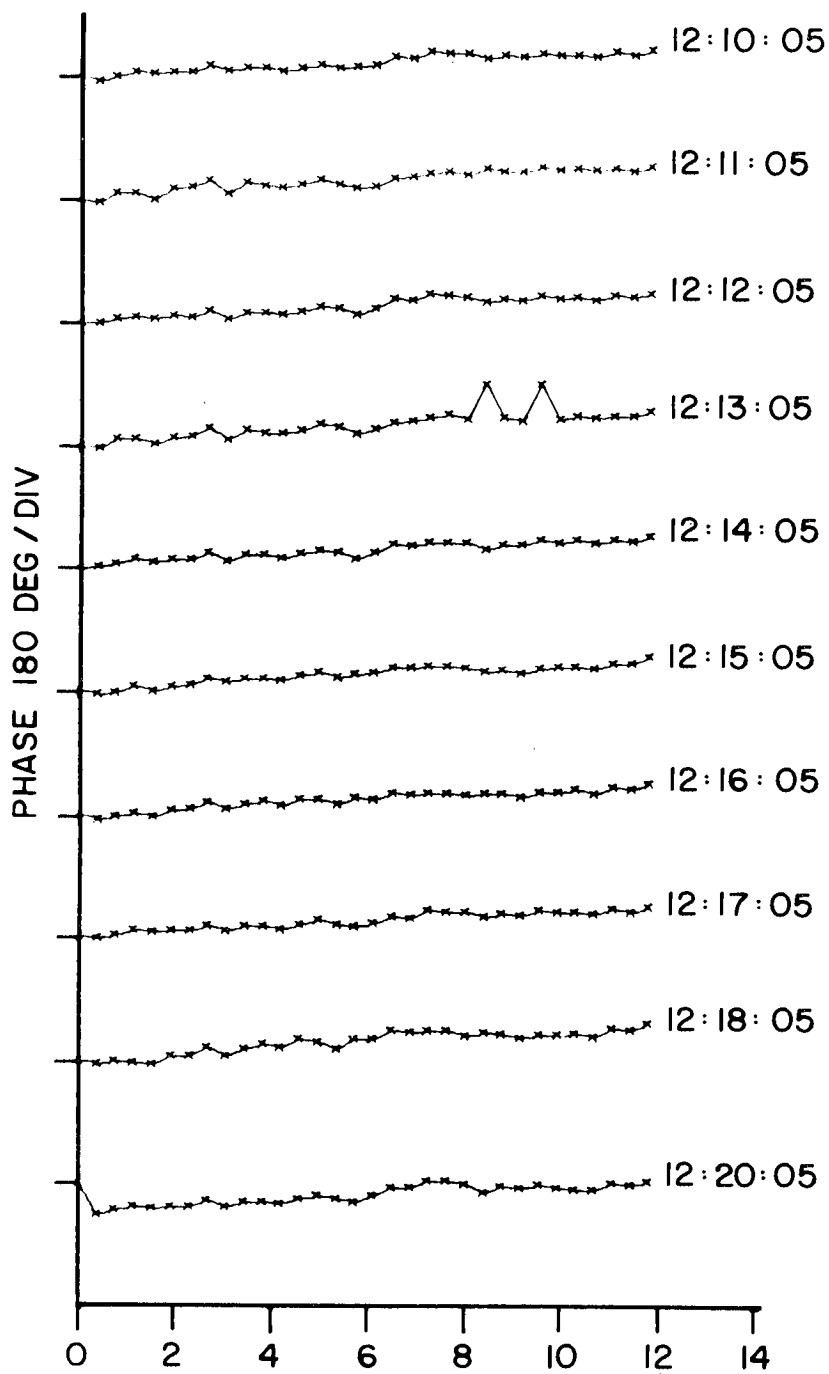
Figure 8. Phase Front Plots for Site 1
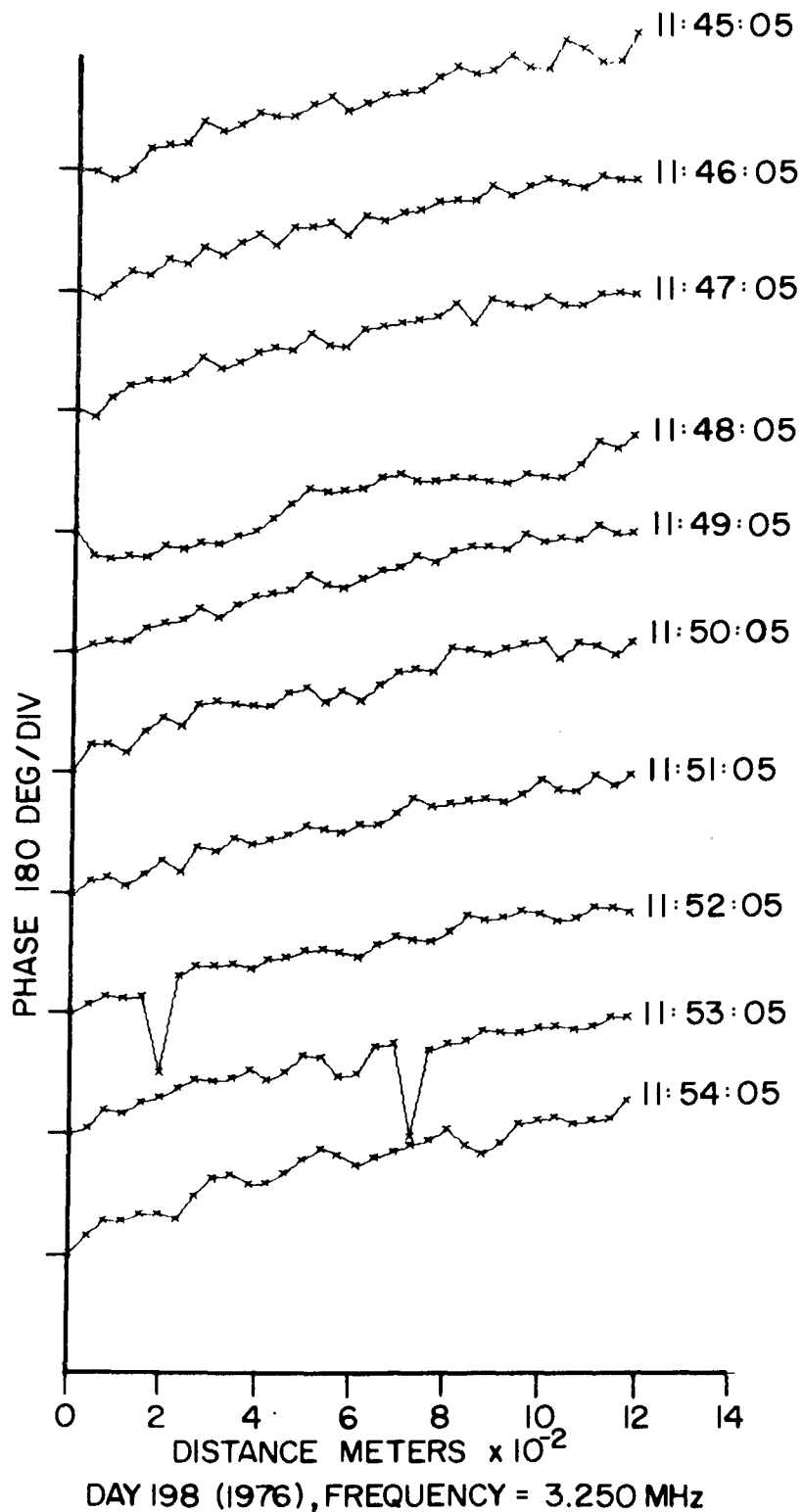
Figure 9. Phase Front Plots for Site 1

Figure 11. Phase Front Plots for Site 7

Occasionally the value of a phase was bad. An example of this may be seen in Figure 10 for time 12:13:05. When this happened the data for that wave front was excluded from the calculations.

Also, occasionally, the phase plot showed marked deviation from a smooth curve. This is illustrated in the phase plot for time 11:48:05 in Figure 11. It is believed that this phenomenon is due to interference between the direct ground wave and a wave that had the same source as the ground wave but was reflected from a moving object such as an airplane or a moving vehicle. These phase fronts were not excluded from the calculations.

The signal to noise ratios (SNR) were estimated by two methods. In the first method the formula

$$SNR = 1/(\text{rms phase error in radians}) \qquad (43)$$

was used[1]. The estimated SNR's are given in Table 4.

TABLE 4

SNR (dB) as Estimated by Equation (43)

Site	3.25 MHz	5.25 MHz	10.35 MHz
1	25	21	20
2	24	23	—
3	23	22	21
4	22	22	19
5	22	21	20
6	20	20	10
7	22	20	12

In the second method the SNR was estimated by comparing, in the Fourier transformed data, the amplitudes of the signal components with the amplitudes of the components which represented the background noise. Table 5 gives the SNR for each site and for each frequency as estimated by this method. Since the resolution of the component levels was 3 dB, each entry in Table 5 is subject to an error of ± 6 dB.

TABLE 5

SNR ± 6 dB as Estimated from Signal Amplitudes and Noise Amplitudes

Site	3.25 MHz	5.25 MHz	10.35 MHz
1	54	54	42
2	51	51	—
3	51	51	30
4	21	36	23
5	33	30	27
6	21	24	9
7	24	27	12

The two methods of estimating SNR gave similar values for the more remote sites for which SNR was low. For the nearer sites, however, the method which uses signal amplitudes and noise amplitudes gave much higher values of SNR. It is likely that this method gives the more accurate estimates since the values for SNR which were found by this method vary more or less uniformly from a high SNR for the near sites to a low SNR for the site which are farthest away. The low values of SNR for the near sites, as predicted from the rms phase errors, would be due to systematic errors in the measurement of the phase values.

8.2 RESULTS OF THE EXPERIMENT

The ranges which were computed for each site by processing the phase front data are given in Table 6. Each Figure in that table is the mean of all the results for a given site and a given frequency while the figures which are expressed as errors are the rms deviations from the means.

TABLE 6
Estimations of Ranges

Site	True Range (km)	Mean of Estimated Ranges ± rms Deviation from Mean (km)		
		3.25 MHz	5.25 MHz	10.35 MHz
1	13.38	13.72 ± .03	11.66 ± .01	12.95 ± .03
2	21.69	19.13 ± .08	21.18 ± .07	—
3	37.42	30.10 ± .17	32.00 ± .17	36.71 ± 2.32
4	56.46	45.87 ± 14.55	45.80 ± 2.26	52.73 ± 3.37
5	74.15	51.89 ± 3.06	56.29 ± 4.80	63.47 ± 4.48
6	87.42	84.58 ± 34.11	58.59 ± 2.67	86.87 ± 31.93
7	111.46	103.6 ± 31.4	105.16 ± 37.49	120.4 ± 51.2

Table 7 shows the percent bias in the estimated ranges plus or minus the rms deviation from the mean expressed as a percentage.

TABLE 7
Errors in Estimations of Ranges

Site	Percent Bias ± Percent rms Deviation from the Mean Range		
	3.25 MHz	5.25 MHz	10.35 MHz
1	+ 2.5 ± 0.22	−12.9 ± 0.09	− 3.2 ± 0.23
2	−13.0 ± 0.42	− 2.3 ± 0.33	—
3	−19.6 ± 0.56	−13.5 ± 0.53	− 1.9 ± 6.32
4	−18.8 ± 31.7	−18.9 ± 4.93	− 6.6 ± 6.39
5	−30.0 ± 5.9	−24.0 ± 8.53	−14.4 ± 7.06
6	− 3.2 ± 40.3	−33.0 ± 4.56	− 0.6 ± 36.7
7	− 7.0 ± 30.3	− 5.6 ± 35.6	+ 8.0 ± 42.5

From Tables 6 and 7 the following observations may be made:

i)   The mean of the range estimates is almost always less than the true range.

ii)   There is considerable spread in the bias (from -33% to + 8%) which is interpreted to be statistical variation only; there is no obvious trend as the transmission site is moved from the nearer to the more remote locations.

iii)   The percent rms deviation from the means of the range estimates tends to be smaller for the shorter ranges and larger for the longer ranges.

iv)   Among the lower ranges the rms deviations from the means tend to be much smaller than the deviation of the mean itself from the true range.

v)   The bias is usually negative. This is in contrast to the results of the simulated experiments where it was usually positive.

vi)   The bias is quite different for different frequencies and for different sites. Thus systematic errors and site errors which are constant during continuous operation of the equipment, when no adjustments are made, are larger than the minute to minute fluctuations in the signal itself.

For comparison, the ranges were also computed from a_{1M} and a_{2M}, where these parameters were computed from the a_1 and the a_2 of all sets of data for a given frequency from a given site. This was done because there is better theoretical justification for using a_{1M} and a_{2M} to compute a range than there is for taking the mean of the individual estimates of range. (cf equations (35), (37), and (39) and the associated discussion). The results are given in Table 8. When the rms deviation from the mean is low in Table 6 the estimated ranges in Table 8 are about the same as those in Table 6. When the rms deviation from the mean is high the estimated ranges in Table 8 are lower than those in Table 6. In this case they deviate more from the true range.

TABLE 8

Ranges Estimated from a_{1M} and a_{2M}

| | | Estimated Ranges (km) | | |
Site	True Range (km)	3.25 MHz	5.25 MHz	10.35 MHz
1	13.38	13.72	11.66	12.92
2	21.69	19.13	21.18	--
3	37.42	30.10	32.31	37.49
4	56.46	49.45	45.64	52.50
5	74.15	51.66	51.05	63.17
6	87.42	75.174	51.89	77.72
7	111.46	98.30	96.77	105.16

The estimated values for the directions of the transmission sites were all within 1.1 degrees of the true direction. Table 9 shows the mean of the estimates of the direction for each site and for each frequency. Also, the rms deviations from the mean are shown in that table. In most cases the deviation of the mean of the direction from the true direction is greater than the rms deviation from the mean. This shows again that the system errors are greater than the minute to minute fluctuations in the signal.

TABLE 9

Estimations of Directions With Respect to End of Array

Site	True Direction (Deg.)	Mean of Estimated Direction ± rms Deviation from Mean (Deg.)		
		3.25 MHz	5.25 MHz	10.35 MHz
1	93.38	92.92 ± .00	93.45 ± .00	93.08 ± .02
2	92.32	93.35 ± .01	93.38 ± .01	—
3	91.91	92.23 ± .01	92.29 ± .01	92.17 ± .02
4	91.50	91.67 ± .11	91.73 ± .02	91.66 ± .04
5	90.99	91.21 ± .05	91.24 ± .02	91.18 ± .05
6	90.72	90.68 ± .15	90.91 ± .03	90.79 ± .11
7	91.08	90.95 ± .15	91.05 ± .09	91.02 ± .13

8.3 DISCUSSION OF EXPERIMENTAL RESULTS

In Figures 12 and 13 the curves are the rms deviations from the mean ranges as interpolated from the simulated experiments with the use of Figure 7. For these curves the standard deviation of the phase error was assumed to be 3°. The crosses are the value from the field experiment. The experimental values are sometimes much greater than the predicted values and sometimes much less.

These results may be explained as follows. Systematic errors appear to be present but to be fairly constant during each ten-minute period in which measurements were taken. These errors may produce a substantial range bias (up to 33%) regardless of the SNR. For the near sites the signal is much higher than either the noise, or any interfering signal, so the results are reproducible from minute to minute. This yields a low rms deviation from the mean range. For the more remote sites the signal is lower and noise will have a greater effect. Sometimes the noise level is high which leads to a large rms deviation from the mean range, and sometimes it is low when the rms deviation from the mean range is again small.

8.4 USEFULNESS OF THIS METHOD

For the conditions under which the field experiment was carried out, this method could be used to estimate ranges of up to about 50 km with an error of up to 20%. If the interference is low it could be used for ranges up to 100 km with an error up to about 33%. Above a range of 100 km the low SNR and the sensitivity to interference would make the method of little use.
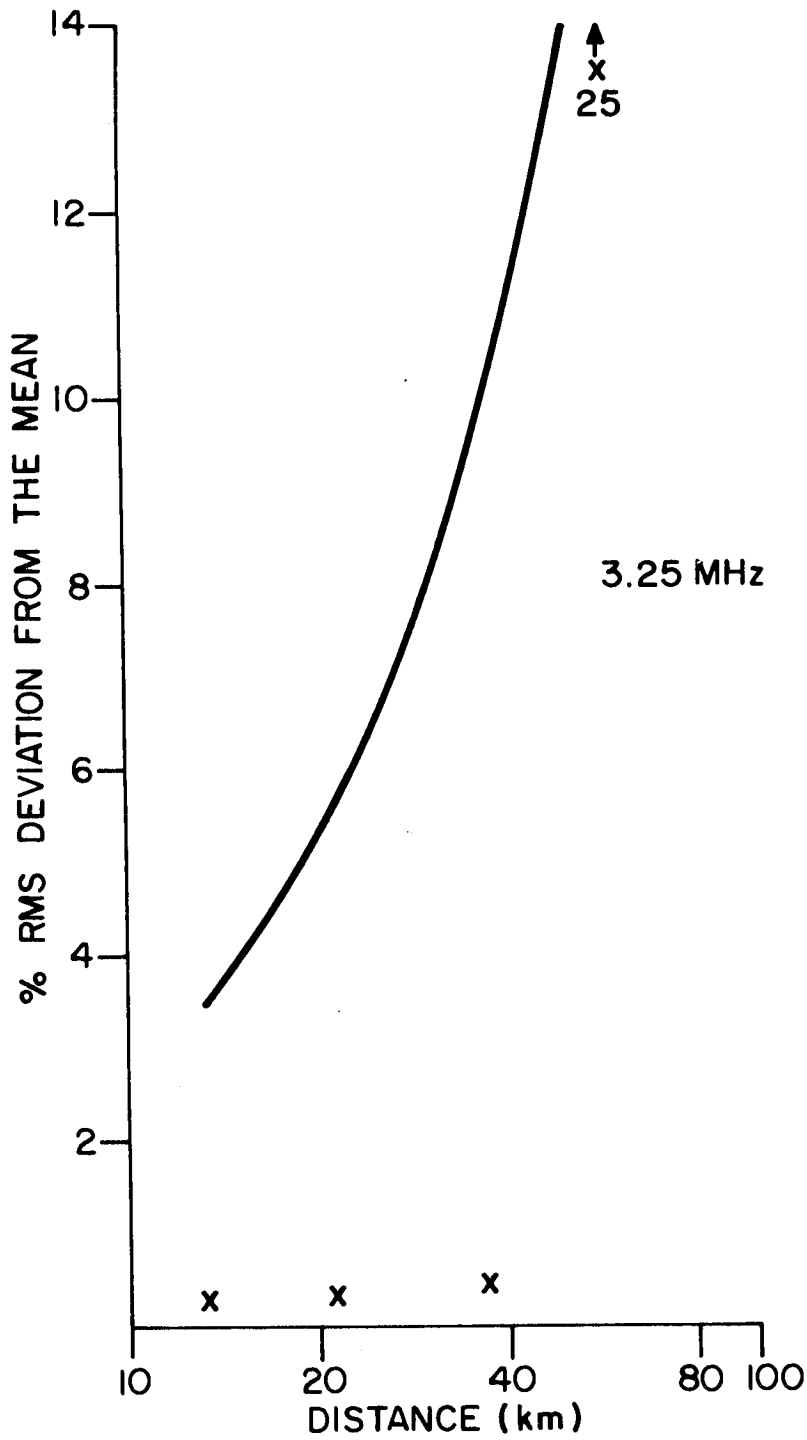
Figure 12. Percent Rms Deviation of R/d from its Mean; A Comparison of Predicted Values (Line) and the Experimental Values (Crosses) 3.25 MHz
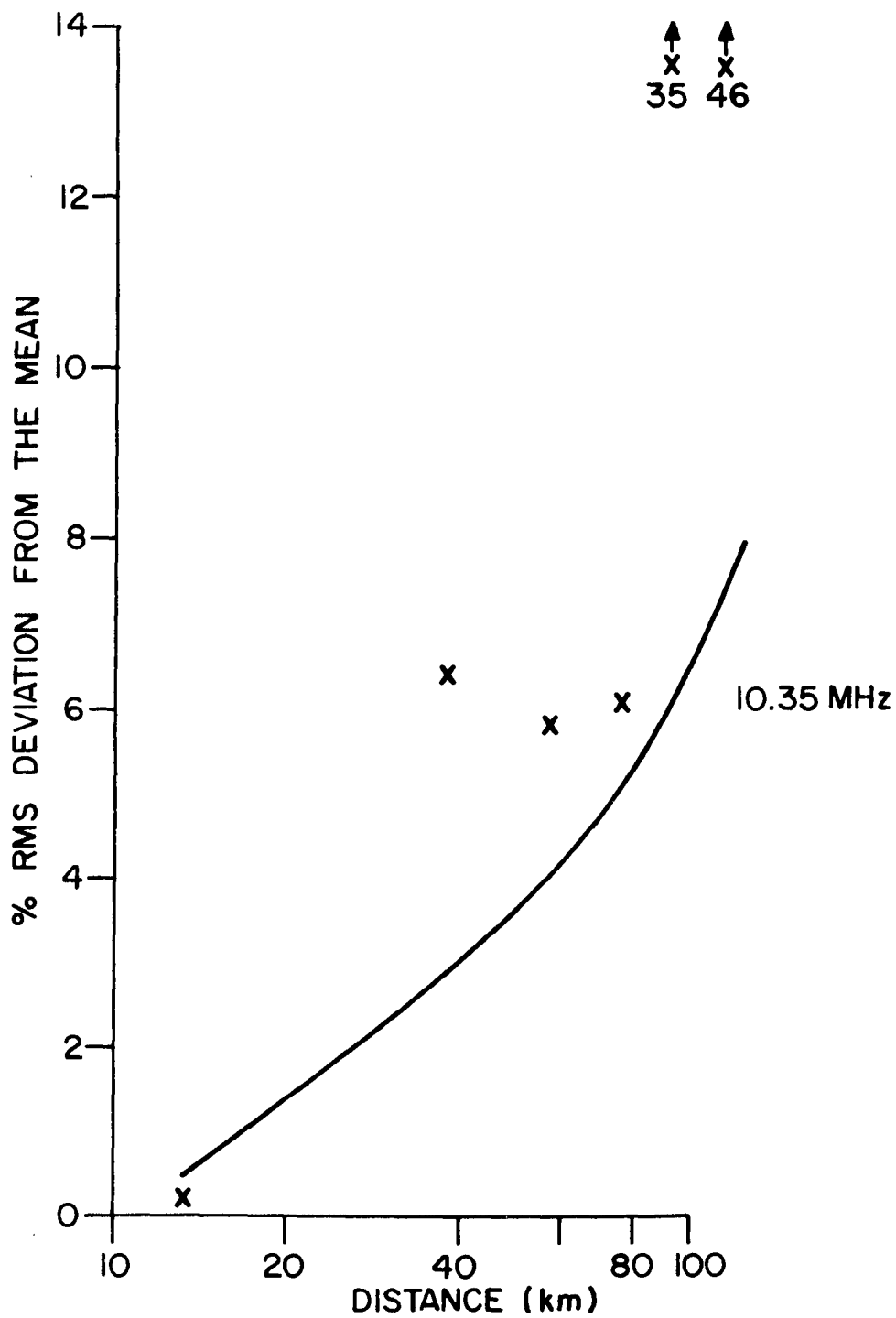
Figure 13. Percent Rms Deviation of R/d from its Mean; A Comparison of Predicted Value (Line) and
the Experimental Values for 10.35 MHz

9. COMPUTATIONS USING VERTICAL INCIDENCE DATA

Computations were carried out using some vertical incidence data which were taken at the HFDF facility at CRC.

For these experiments loop antennas were used with an FMCW signal at a mean frequency of 2.55 MHz. On the basis of travel time, the reflection from the E-layer was separated from the reflections from the other ionospheric layers. On the ionogram the trace of E-layer showed as a clean discrete echo, well separated from the traces of the other layers. This layer was at a height of about 112 km so the total round trip distance, from transmitter to receiver, was about 225 km.

A total of 48 sets of vertical incidence data were processed which were taken at one minute intervals. Of these, 27 sets gave *negative* values for the range. The values scattered between -5500 km and +26000 km with about 90% falling between -1000 km and +1000 km.

The randomness in these results may be explained as follows. The E-layer has irregularities in it so the surface which reflects a signal of a given frequency would be rough rather than smooth. There would, therefore, be focusing effects, multiple reflections, and reflections as slightly different heights; all of which could cause wave interference at the receiver. For example, for two signal rays of 2.55 MHz frequency, a difference in the reflection heights of 30 meters would make them 180° out of phase at the receiver. And since the irregularities in the ionosphere are constantly changing, the wave interference pattern at the receiver would be constantly changing. It follows that the curvature of the wavefront over the aperature would be constantly changing. This results in the range estimates being quite random. Thus, wavefront curvature cannot be used to estimate the range of a signal which is reflected from the ionosphere. Another factor in these experiments is that the round-trip distance of the signal was about twice the predicted useful limit of the method.

10. SUMMARY

The possibility of computing the range of a signal from its wavefront curvature has been investigated. Many simulated experiments were carried out. Some success was had by fitting a truncated power series to the data. For noisy data only the terms up to and including the second order term were used. The use of higher terms gave no improvement. For range estimates the percent bias and the percent rms deviation from the sample mean were plotted against range. The range estimates are better when the signal is broadside to the array than when it is close to endfire.

In a field experiment the ground wave was used to estimate ranges of up to 111 km. A bias of up to 33% was found. It was almost always negative and was attributed to system errors. Sometimes the rms deviation from the mean range was large, up to 42%. This was attributed to noise. But sometimes the rms deviation from the mean was low, much lower than the bias. This was especially true for the shorter ranges. For these cases the signal level would be much higher than the level of the noise.

An attempt to compute the range of a signal, which had been reflected by the E-layer of the ionosphere, was unsuccessful. The range was about twice the useful limit of this method and the return signal may well have consisted of two or more interfering rays.

11. REFERENCES

1.   Rice, D.W. and Winacott, E.L., *A Sampling Array for HF Direction-Finding Research*, CRC Report 1310, November, 1977.

2.   Hayden, E.D., *Propagation Studies Using Direction-Finding Techniques*, Journal of Research of the National Bureau of Standards, Vol. 65D, p. 197, (1961).

A P P E N D I X   A

Derivation of Least-Squares-Best-Fit Equations/ Equations (11) in Text

Let N be the number of antennas in the array and let the phase datum for antenna i, i = 0, 1, ..., N-1, be y_i. The problem is to fit the series

$$y = a_o + a_1 i + a_2 i^2 + \ldots a_M i^M \tag{A1}$$

to these data by method of least squares; that is, we wish to choose $(a_o, a_1 \ldots a_M)$ such that

$$\sum_{i=0}^{N-1} (y-y_i)^2 = \sum_{i=0}^{N-1} (a_o + a_1 i + a_2 i^2 + \ldots a_K i^k + \ldots a_M i^M - y_i)^2$$

$$(k = 0, \ldots, M) \tag{A2}$$

and

$$\frac{\partial}{\partial a_k} \sum_{i=0}^{N-1} (y-y_i)^2 = 2 \sum_{i=0}^{N-1} (a_o i^k + a_1 i^{1+k} + \ldots a_k i^{k+k} + \ldots$$

$$a_M i^{M+k} - y_i i^k). \quad (k = 0, \ldots, M) \tag{A3}$$

$$= 0 \tag{A4}$$

where we define 0^0 to be one.

The right sides of equations (A3) and (A4) can be written as

$$a_o T_k + a_1 T_{1+k} + a_2 T_{2+k} + \ldots a_k T_{k+k} + \ldots a_M T_{M+k} = Y_k$$

$$k = 0, \ldots, M) \tag{A5}$$

where

$$T_j = \sum_{i=0}^{N-1} i^j \tag{A6}$$

$$Y_j = \sum_{i=0}^{N-1} y_i i^j \qquad (A7)$$

Letting k = 0, 1, ...,M equation (A5) can be rewritten as the set of equations

$$a_o T_o + a_1 T_1 + a_2 T_2 + \ldots a_M T_M = Y_o$$

$$a_o T_1 + a_1 T_2 + a_2 T_3 + \ldots a_M T_{M+1} = Y_1$$

$$a_o T_2 + a_1 T_3 + a_2 T_4 + \ldots a_M T_{M+2} = Y_2$$

.

. $\qquad (A8)$

.

$$a_o T_M + a_1 T_{M+1} + a_2 T_{M+2} + \ldots a_M T_{2M} = Y_M$$